

Laboratory Investigation of Air Turbulence above Simple Water Waves¹

R. J. LAI AND O. H. SHEMDIN

University of Florida, Gainesville 32601

The structure of turbulent-shear flows above propagating waves is investigated experimentally in a wind and wave facility at the University of Florida. Wave-induced perturbations and their importance in transferring momentum to waves is a central question in this study. The turbulent air velocities were measured in the horizontal and vertical directions by using a two channel hot-film anemometer system. Turbulence measurements were obtained both in the presence and absence of mechanical waves with wave height = 8.9 cm and wave speed = 2.23 m/sec. Power spectra of air turbulence indicate the presence of significant wave-induced peaks in both the horizontal and vertical velocities at the frequency of mechanical wave. The peaks disappear in the absence of mechanical waves. Calculations of momentum transfer to waves based on the wave-induced Reynolds stress and on the measured growth rate of waves indicate that the interaction of surface waves with the turbulent flow above them produces significant momentum transfer in addition to the wave-induced stress.

When a turbulent air stream blows over water, it generates waves that grow with time and fetch. The waves modify the turbulent properties of the air which in turn modify the rate of energy transfer to waves. The interaction between a turbulent air stream and surface waves is a central problem which has been under intensive study during the past decade with the aim of arriving at a rational basis for wave forecasting. The nature of the interaction between air flow and surface waves in the thin layer immediately above the air-sea interface has been the subject of theoretical controversy. On the one hand, the theory of *Phillips* [1957] is based on the assumption that energy transfer to waves is brought about by advected eddies which remain unaffected by waves. The transfer takes place by a resonance mechanism between waves and the advected eddies that travel with the wave speed. On the other hand, the theory of *Miles* [1957] is based on a complete interaction between surface waves and the shear flow in air. No turbulent eddies are considered to interact with the water surface. The perturbation in the air flow is dependent on the surface waves. In this theory, energy transfer to waves

takes place at a 'critical layer' height which is the height at which the wind speed equals the wave speed.

Laboratory and field evidence up to date indicate that neither of the above two theories is entirely correct. Rather, the degree of the interaction and feed back between a turbulent air stream and surface waves varies depending on the wind velocity compared to wave celerity. The interaction may range from a one way coupling, as suggested by *Phillips* [1957], in the early stage of generation, to a two way coupling between the air flow and surface waves in the stage of rapid growth.

The experimental evidence on the nature of air-sea interaction has not been consistent. *Smith* [1967] measured wind turbulence over the ocean by a thrust-anemometer and did not report turbulent peaks at the peak frequency of surface waves. This was amplified in a discussion by *Stewart* [1967]. *Ruggles* [1969], however, reported strong interaction between ocean waves and wind turbulence which he measured by hot-film sensors. In the laboratory, spectra of turbulence were obtained by *Hess et al.* [1968]. The latter spectra showed no peaks to correspond to peaks in the surface-wave spectra. More recently, *Kato and Sano* [1969] presented results that show such peaks at the frequency of mechanically generated surface waves. Both *Ruggles* [1969] and *Kato and*

¹ Presented at the Fifty-first Annual Meeting of the American Geophysical Union, Washington, D. C., April 1970.

Sano [1969] took special care in selecting narrow-frequency bandwidths in their spectral computations. The first author used a spectral bandwidth of 0.025 Hz and the latter authors used 0.1 Hz. When the bandwidth is large, the power is averaged over neighboring frequencies; consequently the peaks, such as those that may result from interaction between waves and wind, are suppressed. The discrepancy between the results of above investigators appears to be due to analysis of data rather than physical processes.

The purpose of this study is to shed light on the discrepancy regarding the nature of interaction between wave and wind and to establish the degree of interaction under different wind speeds relative to wave speed. The study is based on direct measurement of the horizontal and vertical components of turbulence at different fetches and elevations above the mean water level. Use was made of a mechanical wave generator to study the structure of turbulence above the water surface in the presence and absence of mechanical waves. A turbulent shear flow in air was generated by passage over a rough transition plate and through a rack on which horizontal bars were set at preselected spacings. The initial turbulence level and distribution were measured and their modification by surface waves downstream were detected.

The properties of turbulence above a propagating wave made of a pliable boundary were reported by *Kendall* [1970]. The wave speed was controlled by selecting the frequency of the movable elements, which were set with specified phase lags to produce a propagating wave. The waves did not always satisfy the dispersion relationship associated with surface waves. The results, however, indicated strong interaction between the turbulent wind and the propagating wave. *Karaki and Hsu* [1968] investigated the wave-induced Reynolds stress above propagating waves. Their results indicated the importance of wave induced perturbation and suggested the need for further investigation.

EXPERIMENTAL APPARATUS AND PROCEDURE

Wind-wave facility. The wind-wave research facility at the University of Florida was described in detail by *Shemdin* [1969b]. Briefly, the wave channel is 1.83 meters wide and 45.7 meters long, and is divided into two bays of equal

width. The height of the facility is 1.93 meters. One bay is provided with a roof and is used as a wind channel. The water depth is maintained at 91.5 cm by a small electrically controlled water pump. The air intake is modified to simulate rough turbulent air flow in the wind channel. The wind intake is shown in Figure 1a. In addition to the honeycomb, the air intake is provided with a grid with preselected solidity distribution, i.e., rows of 1.77-cm rods placed at different spacings such that a preselected shear stress is generated in the turbulent field. This procedure was used by *Rose* [1965] to develop a homogeneous shear flow. The intake is also provided with a 2.42-meter long transition plate on which rows of square transverse bars with a height of 3.8 cm are spaced at 45.7 cm along the plate. This insures a thickened boundary layer and a roughwall flow before interacting with the mechanically generated waves. The height and spacing of the bars were selected based on a study by *Liu et al.* [1966]. The normalized turbulent intensities $((u'^2))^{1/2}/U_\infty$ and $((w'^2))^{1/2}/U_\infty$ were found to be 6% and 4%, respectively, before interaction with water surface, where u' refers to the component along the direction of wave propagation, w' refers to the component normal to mean water surface, and U_∞ refers to the free stream velocity.

Instrumentation. The mean air velocities were measured by a pitot-static probe manufactured by United Sensors and Control Corporation. A probe with a 0.318-cm diameter was placed in the free stream above the transition plate to measure reference velocities U , as shown in Figure 1a. Another probe, 0.159-cm diameter, was used at the test stations to measure mean velocity profiles. A Pace differential pressure transducer (model P90D) was used to measure pressure differences of the pitot-static probe. The transducer was calibrated by a precision micromanometer manufactured by Texas Instruments, Inc.

The fluctuation of air velocities was measured by a hot-film anemometer system. A three-channel constant temperature system (Thermo-Systems, Inc., model 1050) with linearizers (model 1055) was used in this study. The cylindrical quartz-coated hot-film sensors manufactured by Thermo-Systems, Inc. (model 1241-20) were used to measure the two dimensional velocity structure. The cylindrical sensors were

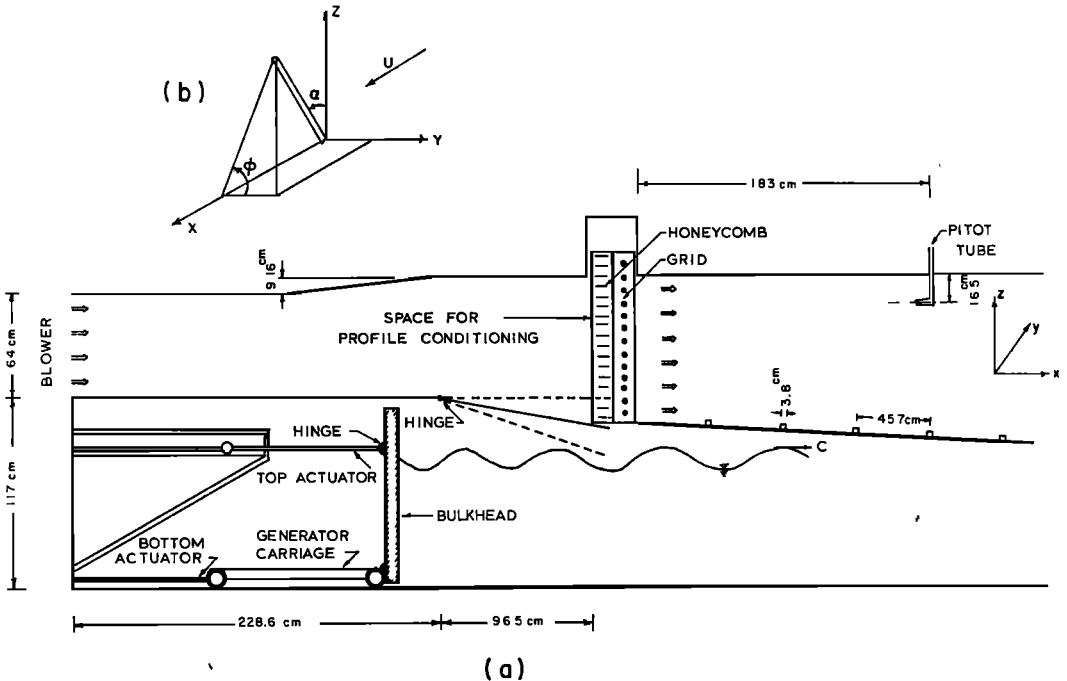


Fig. 1. The side view of the air intake is indicated by (a). The sensor alignment definition sketch is indicated by (b).

0.0508 mm in diameter and 1.016 mm in length and had needle supports with gold plate mounting. A correlator (model 1015C) and a true RMS meter (model 1060) were used with the system.

A calibration wind tunnel was built from a section of 20.3-cm diameter pipe to test and calibrate the hot-film anemometer system. The hot-film sensors were set inside the core flow of the pipe and calibrated in reference to a pitot-static probe. Each sensor was independently adjusted normal to the flow for calibration. A vertical traverse mechanism was developed on which the cross-film sensors were mounted and placed at various elevations above the mean water level. The sensors were mounted on a shaft which could be adjusted for tilt, lateral alignment, and rotation about its axis.

The following three factors were considered in evaluating the errors associated with turbulent measurements by means of hot-films.

1. Accuracy of electronic linearization. This was tested in the calibration wind tunnel. Linearity was achieved to within 3% error.

2. Convective cooling. This occurs in hot-films and hot-wire sensors inclined to the direction of mean flow where additional cooling is brought about by the velocity component along the sensor. This effect was studied by Champagne and Sleicher [1967] and Champagne *et al.* [1967] for platinum hot-wire sensors with different lengths l and diameters d .

Convective cooling is conveniently specified by a factor K defined

$$U^2(\alpha) = U^2(0)[\cos^2 \alpha + K^2 \sin^2 \alpha] \quad (1)$$

where α is the sensor angle to mean flow, $U(0)$ is the mean velocity when α is 0° . The factor K specifies the deviation of the wire directional properties from the cosine law. The hot-film sensors used in the present study had $l/d = 20$. The sensors were quartz-coated hot-films with low end conduction losses compared to hot wires. The directional properties were tested in the wind tunnel and K was found to be 0.25. This corresponded to errors in the horizontal intensity, vertical intensity, and Reynolds stress equal to zero, 28%, 13%, respectively, evaluated by Champagne and Sleicher's derivations.

3. Alignment of sensors. A sensor's alignment with respect to the flow can be specified by the vertical plane angle α and another angle in the horizontal plane ϕ . A comprehensive treatment of alignment angles was given by Klatt [1969] who showed that ϕ can be $90^\circ \pm 5^\circ$, without producing significant errors in velocity fluctuations in either x - or z -direction (see Figure 1b). During the experiments, the alignment was maintained at $\phi = 90^\circ \pm 1^\circ$.

The cross-films were placed in planes parallel to the x - z plane. The manufacturer provides cross-film sensors A and B with $\alpha_A = \alpha_B + 90^\circ$ to a high degree of precision. The sensors were placed in the flow so that $\alpha_B = 45^\circ$ and $\alpha_A = 135^\circ$. Significant errors can result if α_B deviates from 45° . To minimize this error, the cross-films were rotated 180° with ϕ corresponding to 90° and 270° . The readings from both sensors were recorded in each position. During calibration α_B was set such that the difference between the mean voltage readings at $\phi = 90^\circ$ and 270° was less than 4%. This corresponded to $\alpha_B = 45^\circ \pm 1^\circ$ and errors in the horizontal and vertical velocities less than 0.1%.

The water surface elevation was measured by a capacitance wave gage made from Nyclad insulated wire. The probe was balanced by a bridge used in conjunction with the carrier-amplifier of an oscillograph recorder (Hewlett-Packard, model 7708B). The relationship between the wave height and the output voltage from the recorder was found linear. The linearity was checked before and after each run to minimize the error.

Experimental procedure. Two series of experiments were performed to investigate the effect of propagating waves on the wind field: one in the absence of mechanical waves and the other in the presence of mechanical waves. Mean velocity profiles and turbulent fluctuations were measured with and without mechanical waves at fetches 9.15 meters (9.15 meters downstream of air intake) and 24.36 meters. The four reference wind speeds selected were $U_r = 1.95, 2.86, 4.57, \text{ and } 10.66$ m/sec. The location of the reference probe is shown in Figure 1a. In the second series, mechanical waves with a wave height $H = 8.9$ cm and a wave speed $c = 2.23$ m/sec were generated. The wind and waves were selected to produce $c > U_r$, $c \simeq U_r$, and $c < U_r$, in order to simulate idealized air-sea inter-

action processes similar to those occurring in the ocean. The velocity components u' and w' and the surface displacement η were measured simultaneously and recorded on magnetic tape for spectral analysis. The RMS values of u' , w' , and η were obtained by analog means using the true RMS meter.

The reference wind speed was recorded continuously during the testing period. The temperatures of air and water were also measured periodically for reference. At each fetch, measurements were obtained at several elevations in the range 8.9 to 50.8 cm above the mean water level. All the measurements in air were obtained by sensors fixed in space with respect to the mean water level.

The velocity measurements reported by Shemdin [1969a] were obtained by sensors which followed the water surface. The total head and static pressure probes used had response characteristics which allowed the accurate measurement of the horizontal wave-induced velocity perturbation, but filtered out the high frequency turbulence. Although considerable insight was gained about the air motion in the trough of waves, the relative magnitude of the wave-induced velocity compared to turbulence intensity could not be determined then. The present investigation is aimed at establishing the latter. The stationary sensors used in this study allow accurate measurement of turbulence in a wide range of frequencies and elevations above the air-water interface but do not allow measurements in the troughs of waves.

Spectral analysis. The recorded data were analyzed spectrally by means of the analog power spectrum analyzer. The mathematical basis of this analyzer was discussed by Shemdin and Lai [1970]. The power and cross-power spectra were analyzed in the frequency range 0.3–200 Hz. The record length used was 200 sec. Two different bandwidths were selected for the analysis. In the frequency range below 10 Hz, the bandwidth 0.2 Hz was used and in the frequency range 10–200 Hz, the bandwidth 2 Hz was used. The first gave 80 degrees of freedom with a confidence limit of 80%. The latter gave 800 degrees of freedom with a confidence limit of 95%. The low-pass filter of the analyzer has a normalization circuit to incorporate the filter bandwidth effect. This permits a uniform output power for different bandwidths (i.e.,

normalized with respect to a selected bandwidth).

EXPERIMENTAL RESULTS AND DISCUSSION

The mean velocity profile. Figure 2 shows the velocity profiles in the absence and presence of mechanical waves at fetch 9.15. The growth of boundary layers on roof, walls, and water surface with fetch has the effect of increasing the free stream velocity with fetch. The increase can be detected both in the presence and absence of mechanical waves. The properties of the profiles shown in Figure 2 and properties of other profiles at fetch 24.36 are summarized in Tables 1 and 2. The mean velocity profiles can be reasonably approximated by logarithmic distributions from which U_* values were determined. The results shown in Figures 2 and Tables 1 and 2 indicate that U_* increased by 15% on the average, due to the presence of mechanical waves. The increase in U_* varied from 2.5% for $U_r = 1.95$ m/sec to 30% for $U_r = 10.66$ m/sec. These results will be discussed further in light of the wave-induced effect on the cross spectra of turbulence above waves. A quantitative analysis of the influence

of waves on the measurement of velocity by a pitot-static probe fixed in space above the mean water level was given by *Shemdin* [1970]. The influence of waves was shown to be due to the periodic change in the water-surface elevation and the wave-induced oscillation of the velocity above the surface. For a turbulent boundary layer it was found that U_* increased due to the presence of mechanical waves. The cases studied had a wind speed greater than the wave speed and the results are consistent with present investigation.

Spectra of water surface displacement. In Figure 3, the energy spectra in the presence of mechanical waves are shown for fetches 9.15 and 24.36. At each fetch, two spectra are shown corresponding to reference velocities $U_r = 1.95$ and 10.66 m/sec. At the low wind speed, the spectra do not show ripples. At 10.66 m/sec the spectrum at fetch 9.15 shows a mild peak at 1.5 Hz and a larger peak at the mechanical wave frequency. At fetch 24.36, a relatively large peak appears at 2.0 Hz which represents the wind generated ripples. The ripples are small at fetch 9.15 but grow rapidly with fetch. The spectra at fetch 24.36 also show a large peak at the mechanical wave frequency. The growth

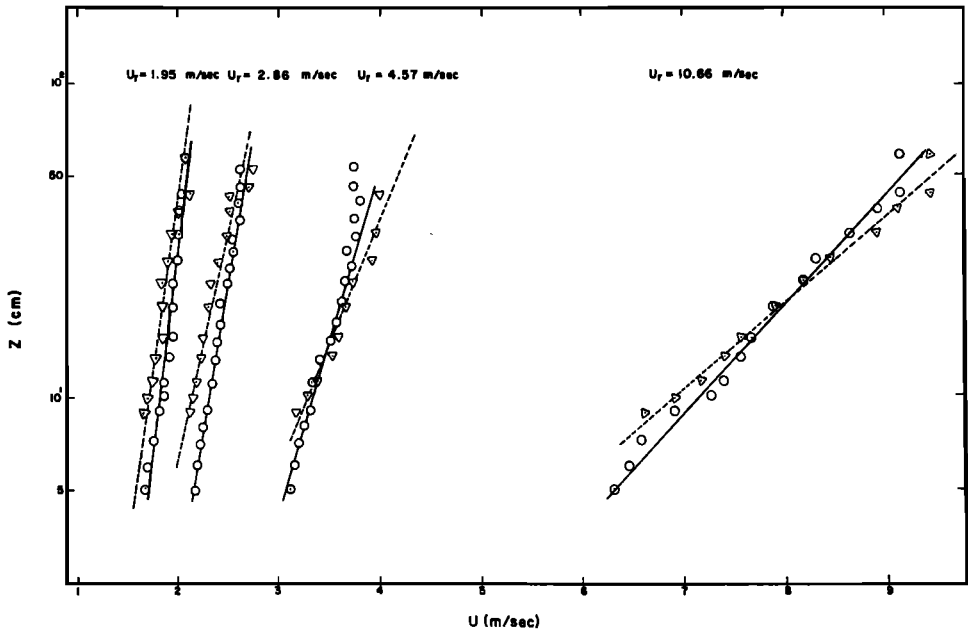


Fig. 2. Mean-velocity profiles at fetch 9.15. Triangles indicate those with mechanical waves. Circles indicate those without mechanical waves.

TABLE 1. Properties of the Mean Velocity Profiles in the Absence of Mechanical Waves

	Fetch 9.15				Fetch 24.36			
U_r , m/sec	1.95	2.96	4.57	10.66	1.95	2.96	4.57	10.66
U_{*} , cm/sec	9.65	10.6	17.4	48.4	9.76	10.7	20.0	59.5
U_{∞} , m/sec	2.07	2.81	3.91	9.25	2.07	2.67	4.08	9.67
U_{∞}/U_{*}	21.4	26.5	22.5	18.7	21.2	24.9	20.5	16.3

and damping of mechanical waves is discussed in detail in a section on wave growth.

Influence of surface waves on air turbulence. In Figure 4 three spectra of w' are compared in the frequency range 0.3–200 Hz. The first was measured at fetch 2.0 with $z = 10.2$ cm above the rough transition plate. It characterizes the horizontal turbulent field entering the test section. The second and third spectra were measured at fetch 9.15 over the water surface, in the presence and absence of mechanical waves, respectively. The latter measurements were obtained at 10.2 cm above the mean water level. The peak at the mechanical wave frequency appears only in the spectrum above mechanical waves. Above 10 Hz, the turbulence level above the rough plate is higher than that above the water surface. The latter is attributed to the fact that mean wind velocity at fetch 9.15 is less than that at fetch 2.0. The rough plate is sloped downward to permit smooth transition of flow above waves thus making the flow area at fetch 9.15 larger than that at fetch 2.0.

The spectra in the range 10–200 Hz appear to have a slope of $-5/3$ which characterizes the inertial subrange of turbulence. These confirm the observations made by *Kato and Sano* [1969] who also found the equilibrium subrange to exist above 10 Hz. *Hess et al.* [1968] obtained turbulence spectra which indicated the presence of the equilibrium subrange above 30 Hz. This may reflect the dependence of the inertial

subrange on the dimensions of the facility. The Colorado State University facility has a 61.0 cm \times 76.1 cm cross section for air flow compared to 91.4 cm \times 107.0 cm at the University of Florida. The rough transition plate used in this study affects turbulence below the inertial subrange only, as suggested by comparison with the results of *Kato and Sano* [1969] who did not use such a plate but whose measurements in the inertial subrange agree with the results of the present study.

The spectra of w' are shown in Figure 5 for the same three conditions described above for w' . A significant peak appears at the frequency of the mechanical wave. The spectra suggest the existence of the inertial subrange in the frequency range 30–200 Hz. The intensity of turbulence above the rough plate is higher than that at fetch 9.15 for the same reasons discussed above.

The results shown in Figures 4 and 5 indicate that the inertial subrange of turbulence is unaffected by the presence of surface waves, which occur in a lower-frequency range. The surface waves perturb the air flow in the frequency range of energy-producing eddies. Further analysis of the wave-induced perturbation is expanded in the frequency range 0.3 to 4.0 Hz to study the structure of wave-induced motion. In this frequency range, the spectra of horizontal and vertical motions w' and w'' will be compared at different elevations, fetches, and wind speeds.

TABLE 2. Properties of the Mean Velocity Profiles in the Presence of Mechanical Waves

	Fetch 9.15				Fetch 24.36			
U_r , m/sec	1.95	2.86	4.57	10.66	1.95	2.86	4.57	10.66
U_{*} , cm/sec	9.89	11.4	20.7	63.2	10.0	13.7	20.2	64.0
C/U_{*}	22.8	19.6	10.9	3.63	22.3	16.4	11.2	3.6
U_{∞} , m/sec	2.07	2.90	4.0	9.46	2.07	2.66	4.13	9.71
C/U_{∞}	1.08	0.859	0.565	0.24	1.08	0.848	0.55	0.231
U_{∞}/U_{*}	20.9	25.4	19.4	15.0	20.7	19.4	20.4	15.4

$$H = 8.9 \text{ cm}; C = 2.23 \text{ m/sec}; k = 1.92 \text{ m}^{-1}.$$

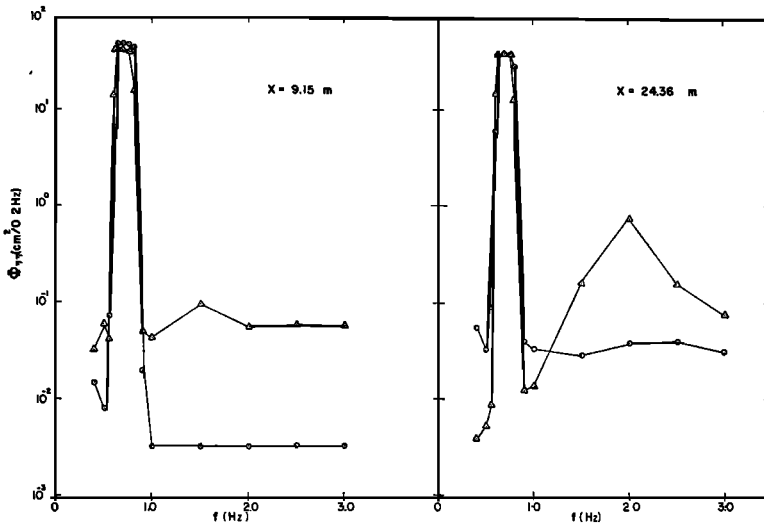


Fig. 3. Spectra of water surface displacements. Circles: $U_r = 1.95$ m/sec; triangles: $U_r = 10.66$ m/sec.

The average of the cross correlation between u' and w' , $\langle(u'w')\rangle$, gives the Reynolds stress. The cross spectrum $C_{u'w'}$ gives the frequency distribution of Reynolds stress. Comparisons will also be made between cross spectra $C_{u'w'}$ at different elevations and wind speeds to investigate the exchange of momentum between wind and waves.

Dependence on elevation. The dependence of power spectra of u' and w' on elevation are shown in Figure 6 at fetch 9.15. The power spectra at elevations 10.2, 20.4, and 50.8 cm are compared for reference wind speeds, $U_r = 1.95$ and 10.66 m/sec. Two main features are recognized. The first is that the wave-induced velocity decreases with height above the mean water level as expected. The second is that the peak at any elevation increases with increasing wind speed. The dependence of the co-power spectra on elevation is shown in Figure 7 at fetch 9.15 for reference velocity 10.66 m/sec. A significant decrease in the magnitude of $C_{u'w'}$ with elevation is observed at the mechanical wave frequency.

The experimental results indicate that the rate of decay of the wave-induced perturbation is more rapid at $U_r = 10.66$ m/sec compared to 1.95 m/sec. This is exhibited clearly by the spectra of w' at different elevations shown in Figure 6. At the high wind speed, the wave-induced spectral peaks are large in magnitude at

low elevation and decrease rapidly with height. At the low wind speed, the peaks are not as large in magnitude but persist at the higher elevations. These results are in accord with the streamline patterns reported by Shemdin [1969a]. At a wind speed that is low compared to the wave speed, the region denoted by the 'matched layer,' where the wind speed equals the wave speed, extends upward a distance of many wave heights above the water surface, whereas at a wind speed that is high compared to the wave speed, the matched layer region is restricted to a distance less than one wave height above the water surface.

Dependence on fetch. In Figure 8, spectra of u' and w' at fetches 9.15 and 24.36 are compared for the reference velocity $U_r = 10.66$ m/sec. The comparison is made for two elevations above the mean water level, $z = 10.2$ and 50.8 cm. The spectra at both elevations show no significant change with fetch. Other results not presented indicated a mild dependence on fetch at higher elevations. The results suggest that the wave-induced velocity perturbation has a negligible dependence on fetch and is perhaps of the same order of magnitude as the variation of wave height with fetch, i.e., small over one wave length but may be significant over a long fetch.

Dependence on wind speed. The dependence of $C_{u'w'}$ on wind speed is shown in Figure 9 for

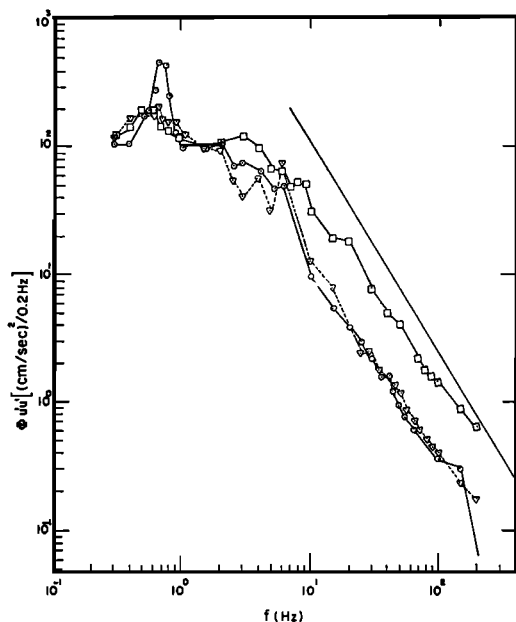


Fig. 4. Spectra of horizontal turbulence in the frequency range 0.3–200 Hz. Squares indicate area above rough plate at fetch 2.0; triangles indicate area above wind waves at fetch 9.15. Solid line has $-5/3$ slope characterizing inertial subrange. $U_r = 10.66$ m/sec; $z = 10.2$ cm.

fetch 9.15 and wind speeds 1.95 and 10.66 m/sec. The results indicate that the direction of momentum transfer is critically dependent on the relative magnitude of wind speed compared to wave speed, C . The latter was maintained at 2.23 m/sec for all wind speeds. At $U_r = 1.95$ m/sec, the results suggest an upward transfer of momentum around the frequency of mechanically generated waves. The direction of momentum transfer is reversed when U_r becomes greater than C , as shown in the same figure for $U_r = 10.66$ m/sec. Two other intermediate velocities $U_r = 2.86$ and 4.57 m/sec were tested. The momentum transfer at the mechanical wave frequency was found to be upward for $U_r = 2.86$ m/sec and downward for $U_r = 4.57$ m/sec. By examining the mean velocity profiles in Figure 2 one may conclude that the direction of momentum transfer depends on the sign of $U_1 - C$ where U_1 is approximately equal to the average wind speed at the average wave-crest level. This result confirms a conclusion made by Deardorff [1967] who also found the wind speed at the average wave-crest level to be

important in momentum transfer. A more recent investigation by Wu [1970] suggests that $U_* - C$ is an important quantity in interactions between wind and waves and that separation takes place from the crest of waves when $U_* - C$ becomes positive. Wu suggests that the organized motion between wind and waves is disrupted by separation which controls transfer in most cases. Wu's conclusions are not entirely consistent with our observations. While separation may occur at $(U_* - C) > 0$, the momentum transfer to waves occurs at $(U_1 - C) > 0$ where U_1 varies from $10 U_* - 25 U_*$. Separation directly influences momentum transfer to high-frequency ripples which have $C \approx U_*$ but only indirectly affects longer waves. The ripples influence the wind profile that is acting over the longer waves and they may interact with the longer waves by nonlinear processes which are not yet completely understood.

The coherence γ^2 between u' and w' is defined

$$\gamma^2 = \frac{[C_{u'w'}^2 + Q_{u'w'}^2]}{\Phi_{u'u'}\Phi_{w'w'}} \quad (2)$$

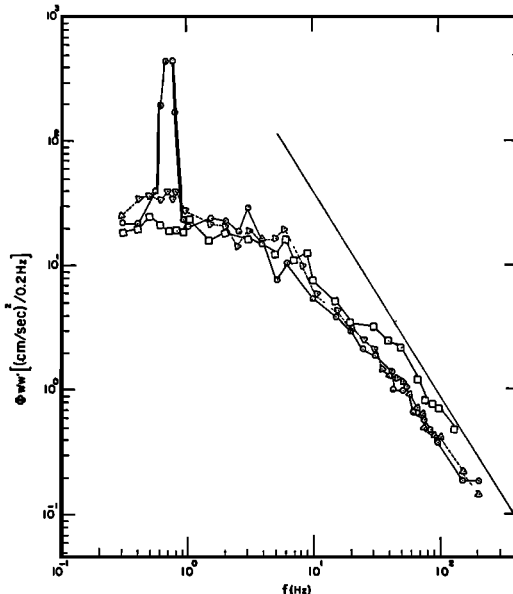


Fig. 5. The spectra of vertical turbulence in the frequency range 0.3–200 Hz. Squares indicate the area above rough plate at fetch 2.0; triangles indicate area above wind waves at fetch 9.15; circles indicate area above mechanical waves at fetch 9.15. Solid line has $-5/3$ slope characterizing inertial subrange. $U_r = 10.66$ m/sec; $z = 10.2$ cm.

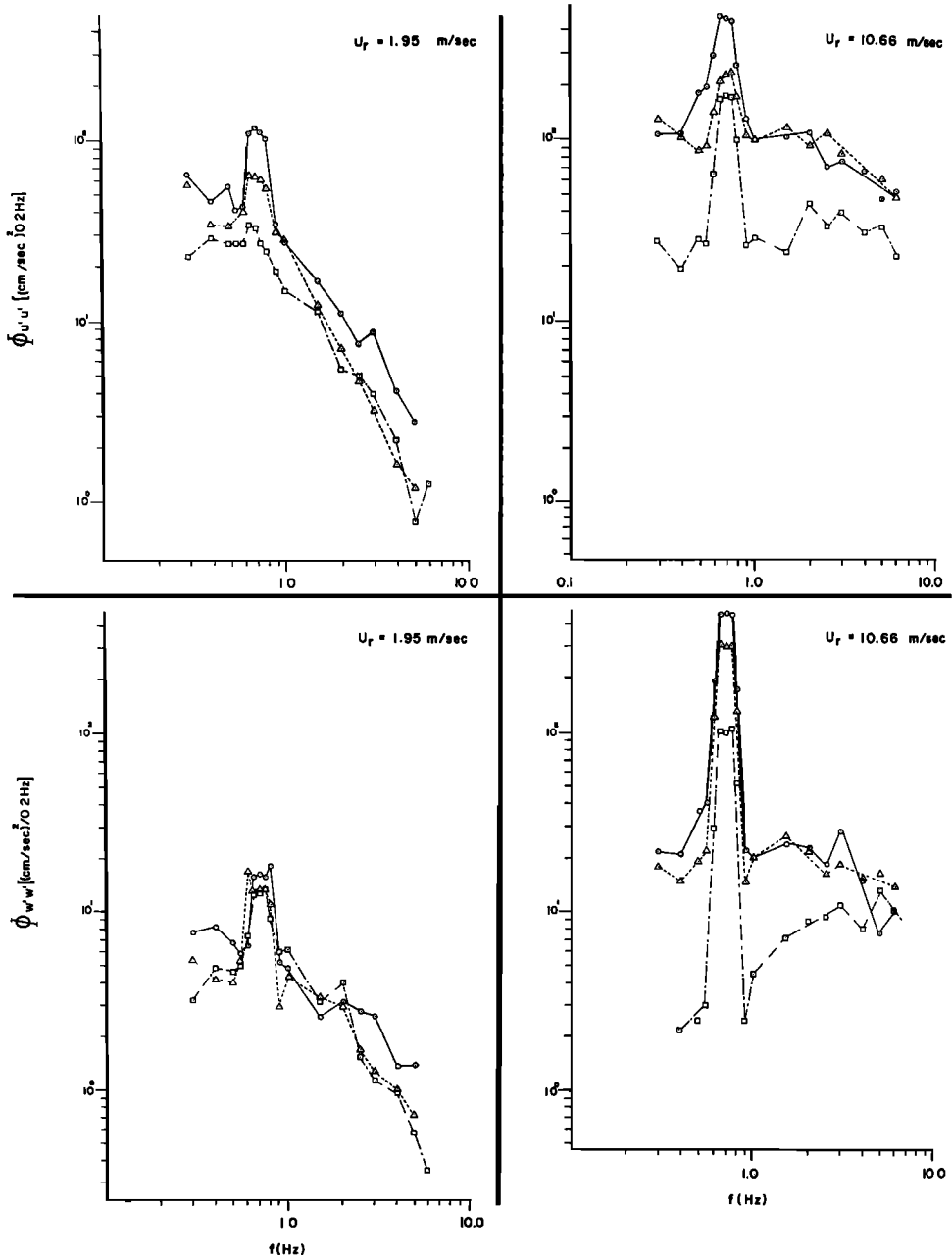


Fig. 6. Variation of power spectra with elevation at fetch 9.15. Circles, $z = 10.2$ cm; triangles, $z = 20.4$ cm; squares, $z = 50.8$ cm.

where $C_{u'w'}$ and $Q_{u'w'}$ are the co- and quad-spectra of u' and w' . The coherence is shown in Figure 9 for both wind speeds $U_r = 1.95$ and 10.66 m/sec. The high coherence level of 0.9 for both velocities suggests a strong direct inter-

action between wind and waves for U_r greater and less than C and confirms the importance of organized motion in momentum exchange between wind and waves.

As mentioned previously, extreme care was

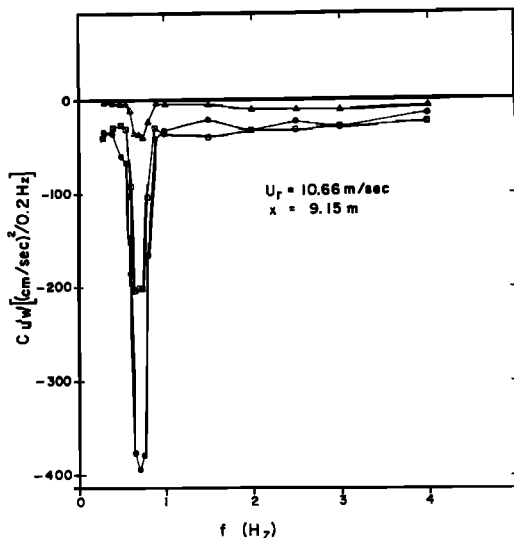


Fig. 7. Variation of co-power spectra with elevation at fetch 9.15 for $U_r = 10.66$ m/sec. Circles, $z = 10.2$ cm; squares, $z = 20.4$ cm; triangles, $z = 50.8$ cm.

taken in alignment of sensors to obtain accurate stresses above waves. Measurements were obtained before and after rotation of sensors and the cross spectra $C_{u'w'}$ were compared to identify accuracy. It was found that the spectra before and after rotation exhibited close agreement at $U_r = 10.66$ m/sec. At the lowest wind speed $U_r = 1.95$ m/sec the spectra before and after rotation showed agreement in the shape of spectra ($C_{u'w'}$ positive in the vicinity of mechanical wave frequency and negative above and below that frequency). The $C_{u'w'}$ values at the mechanical wave frequency deviated by a factor of 2. Such disagreement is not unrealistic considering the low magnitudes of stresses corresponding to $U_r = 1.95$ m/sec compared to those at $U_r = 10.66$ m/sec.

Because of the sensitivity of measurements to alignment of sensors at the lowest wind speed, different experiments are conducted to investigate accuracy of results. Earlier measurements reported by *Shemdin and Lai* [1970] had indicated that $C_{u'w'}$ was positive for all frequencies which is not consistent with basic principles of boundary layer flow. This discrepancy was found to be due to sensor alignment. By proper alignment and rotation, it was consistently found that $C_{u'w'}$ was positive only at the me-

chanical wave frequency and negative elsewhere as expected.

Reynolds stresses above mechanical waves. In Figure 10 the Reynolds stresses $\langle u'w' \rangle$ are shown at different elevations for fetches 9.15 and 24.36 and $U_r = 1.95$ and 10.66 m/sec. The elevation in this figure is normalized with respect to the boundary layer height $\delta_0 = 50.8$ cm. At $U_r = 1.95$ m/sec, $\langle u'w' \rangle$ is very small but mostly positive indicating an upward transfer of momentum. The limits of errors are shown by the brackets in Figure 10. It is seen that the gradient of $\langle u'w' \rangle$ is approximately zero for $U_r = 1.95$ m/sec. At $U_r = 10.66$ m/sec, $\langle u'w' \rangle$ is negative at all elevations indicating a downward transfer of momentum. At fetch 24.36 the variation of $\langle u'w' \rangle$ is approximately linear with elevation which resembles the behavior associated with boundary layers over rigid surfaces. The intensities of u' and w' with and without mechanical waves are compared in Table 3. It is found that the intensities increase consistently at all elevations and wind speeds when the mechanical waves are present.

Previously it was mentioned that the mechanical waves produced an increase in U_* , evaluated from mean velocity profiles, especially at the higher wind speeds. The Reynolds stress is defined

$$-\rho_a \langle u'w' \rangle = -\rho_a \int_0^\infty C_{u'w'}(f) df \quad (3)$$

where f is the wave frequency and ρ_a is air density. In turbulent boundary layers flowing over rigid surfaces, the surface shear stress τ_0 is defined

$$\tau_0 = -\rho_a \langle u'w' \rangle = \rho_a U_*^2 \quad (4)$$

Therefore, it is tempting to attribute the increase in U_* to the added wave-induced motion which appears as a spike in the cross spectrum, $C_{u'w'}$. At the higher wind speeds the results are consistent but at the lowest wind speed, $U_r = 1.95$ m/sec, the reversal in the spectrum at the frequency of mechanical wave suggests a decrease in U_* . The latter is not strongly evident in the mean velocity profiles which suggest a negligible change in U_* . Regardless of the apparent agreement or disagreement indicated above, some doubts remain concerning the legitimacy of equating U_* with $\langle u'w' \rangle$ values above waves especially in view of the type of

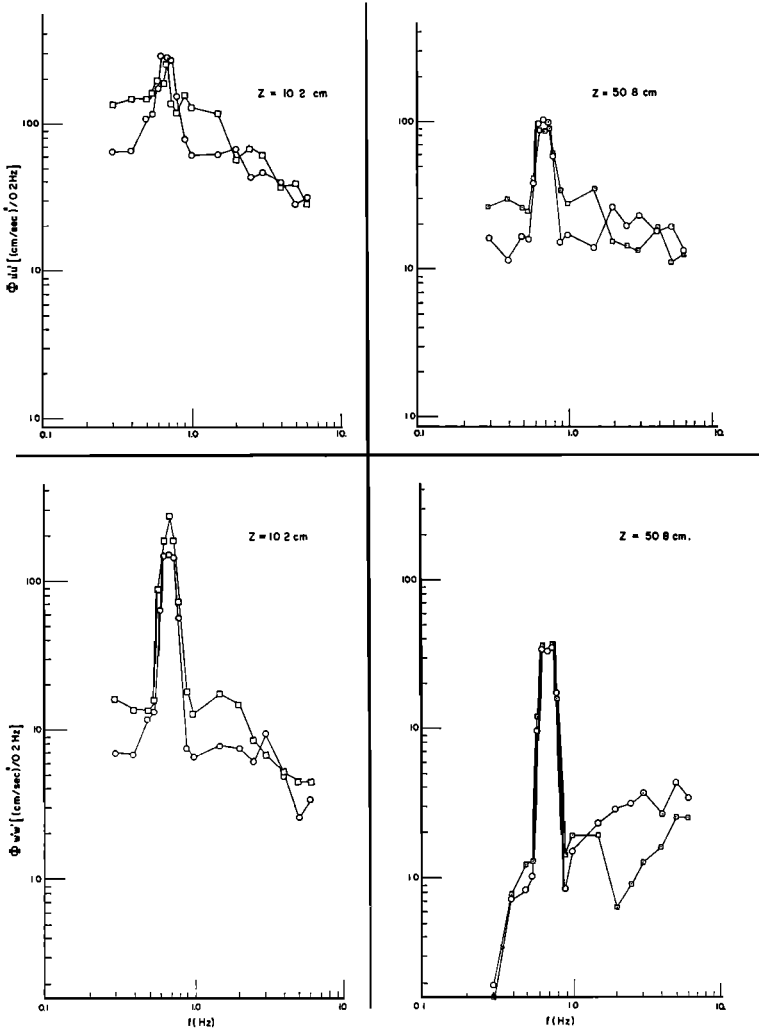


Fig. 8. Variation of power spectra with fetch for $U_r = 10.66$ m/sec. Squares, fetch 9.15; circles, fetch 24.36.

averaging involved in mean velocity measurements by pitot-static probes as discussed by Shemdin [1970]. The U_* values obtained from mean velocity profiles are at best estimates of the mean boundary shear stress. The Reynolds stress measurements $\langle u'w' \rangle$ give more accurate estimates of the boundary stress.

Properties of wave-induced perturbations. The power spectral value at the frequency of the mechanical wave $\Phi_{u'u'}(f_m)$, is a measure of the wave-induced velocity. Also, the phase shift θ obtained from the cross-power spectrum of u' and η is a measure of the phase shift between

the wave-induced velocity and surface displacement η . The dependence of $\Phi_{u'u'}$ and θ on elevation is shown in Figure 11 for $U_r = 1.95$ and 10.66 m/sec for fetch 9.15. The elevation in these figures is also normalized with respect to the boundary layer height δ_0 . The phase shift θ shows a mild dependence on elevation. Its bounds are $140^\circ < \theta < 180^\circ$ for $U_r = 1.95$ m/sec and $-120^\circ < \theta < -40^\circ$ for $U_r = 10.66$ m/sec. This implies that the wave-induced horizontal velocity perturbation lags behind the wave when $U_r = 1.95$ and leads the wave when $U_r = 10.66$ m/sec. Results similar to

these were found with sensors that follow the waves as reported by *Shemdin* [1969a]. Although the phase shifts that were measured then cannot be compared directly to those of the present study, it was also found that the wave-induced horizontal velocity lagged behind the wave when the wind speed was smaller than the wave speed.

The co-power spectrum value at the frequency of the mechanical wave denoted by $C_{u'w'}(f_m)$ is a measure of the wave-induced stress. The phase angle ψ obtained from the cross-power analysis of u' and w' is a measure of the phase shift and reflects the direction of momentum transfer. The profiles of $C_{u'w'}(f_m)$ for $U_r = 1.95$ and 10.66 m/sec are shown in Figure 12 for fetch 9.15. The profiles of phase shift ψ are also shown in the same figure and show a systematic variation of ψ with height. At $U_r = 1.95$ m/sec $-70^\circ < \psi < -20^\circ$ which indicates an upward transfer of momentum at frequency f_m . At $U_r = 10.66$ m/sec $100^\circ < \psi < 180^\circ$ which indicates a downward transfer of momentum at frequency f_m .

Wave growth. The momentum flux to waves

by normal pressure is evaluated by examining the growth rate of waves. Denoting the wave-induced pressure at the surface by ρ

$$\rho = (a + ib)\rho_a g \eta_m \tag{5}$$

where a and b are the normalized in- and out-of-phase components of pressure, ρ_a is air density, g is gravitational acceleration, and η_m is the surface displacement of mechanical wave defined

$$\eta_m = R_e \{ a_0 e^{ik(x-ct)} \}$$

The rate of momentum transfer F is given by

$$F = \left\langle \rho \frac{\partial \eta_m}{\partial x} \right\rangle = \rho_a g k \left(\frac{a_0^2}{2} \right) b \tag{6}$$

where the brackets denote averaging over one wave length in the x -direction.

The rate of increase of wave energy is

$$\frac{dE}{dt} = FC = \rho_a g k \left(\frac{a_0^2}{2} \right) bc \tag{7}$$

where E is the wave energy per unit area

$$E = \rho_w g \frac{a_0^2}{2} \tag{8}$$

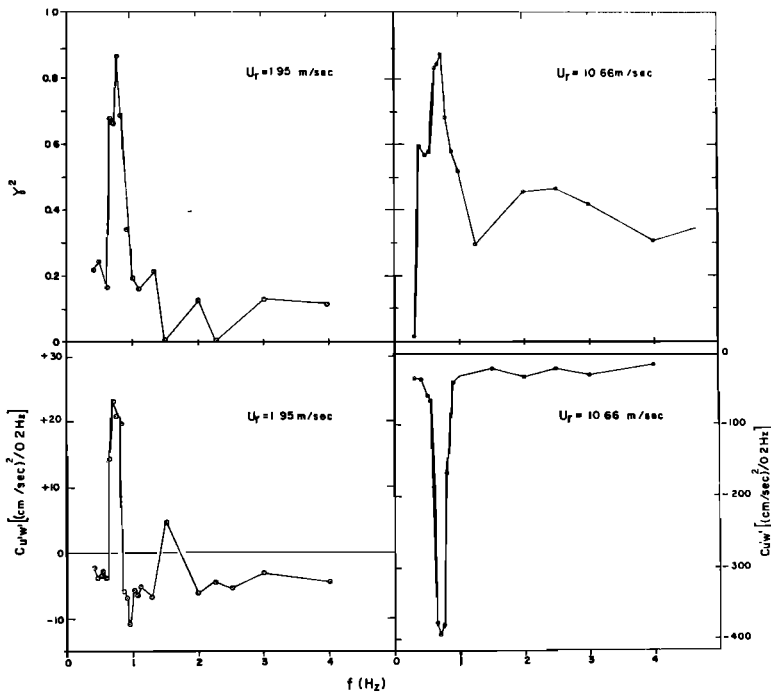


Fig. 9. Dependence of co-power spectra on wind speed for sensors at 10.2 cm above the mean water level and fetch 9.15. The coherence between u' and w' at each wind speed is shown.

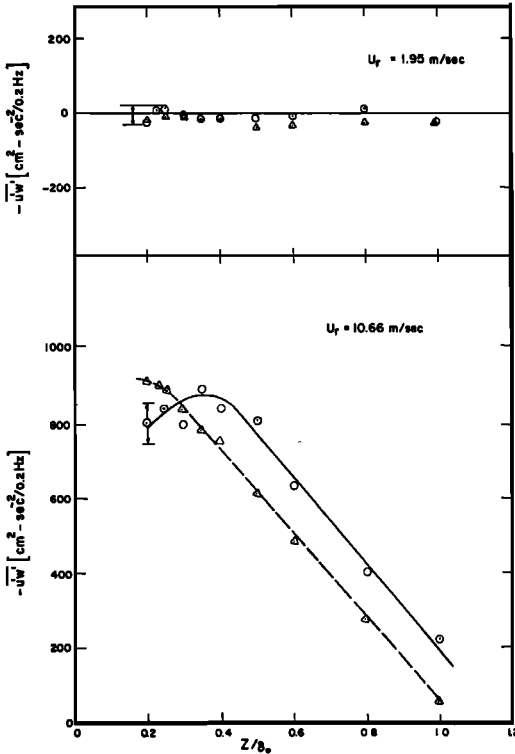


Fig. 10. Variation of the Reynolds stress with $\langle w'w' \rangle$ with height and fetch for $U_r = 1.95$ and 10.66 m/sec. Circles, fetch 9.15; triangles, fetch 24.36.

For a stationary wave system growing in the x direction, equation 7 becomes

$$c_v \frac{\partial E}{\partial x} = \left(\frac{\rho_a}{\rho_w} \right) kc b E \tag{9}$$

so that energy growth is exponential

$$E(x) = E(x_0) \exp \left\{ \left(\frac{\rho_a}{\rho_w} \right) \left(\frac{c}{c_g} \right) bk(x - x_0) \right\} \tag{10}$$

The wave energy for a simple wave n_m can be obtained from spectral results such as those shown in Figure 3. It was shown by Shemdin and Lai [1970] that

$$\Phi_{\eta\eta}(f_m) = \frac{a_0^2}{4} = \frac{E}{2\rho_w g} \tag{11}$$

The spectral growth of wave energy can be expressed

$$\Phi_{\eta\eta}(f_m, x) = \Phi_{\eta\eta}(f_m, x_0) \cdot \exp \left\{ \left(\frac{\rho_a}{\rho_w} \right) \left(\frac{c}{c_g} \right) bk(x - x_0) \right\} \tag{12}$$

The above represents the wave growth due to atmospheric pressure in the absence of damping. In a wave tank damping is expected due to friction at the tank walls and bottom and due to the presence of surface contaminants [Van Dorn, 1966]. Damping produces exponential decay so that a general expression for the rate of change of wave energy with fetch can have the form

$$\Phi_{\eta\eta}(f_m, x) = \Phi_{\eta\eta}(f_m, x_0) \cdot \exp \{ (K_o - K_v)(x - x_0) \} \tag{13}$$

where K_v is a viscous damping factor and

$$K_o = \left(\frac{\rho_a}{\rho_w} \right) \left(\frac{c}{c_g} \right) bk \tag{14}$$

Denoting the ratio of spectral values of fetches x_1 and x_0 , respectively, by R the growth factors can be evaluated from

$$K_o - K_v = \frac{\ln R}{(x_1 - x_0)} \tag{15}$$

where K_o and K_v have the inverse unit dimension as x . The damping factor K_v is determined

TABLE 3. Increase in Turbulence Intensities due to Mechanical Waves

With Mechanical Waves				Without Mechanical Waves		Increase, %	
U_r , m/sec	z , cm	$\langle u'^2 \rangle^{1/2}$, cm/sec	$\langle w'^2 \rangle^{1/2}$, cm/sec	$\langle u'^2 \rangle^{1/2}$, cm/sec	$\langle w'^2 \rangle^{1/2}$, cm/sec	$\langle u'^2 \rangle^{1/2}$	$\langle w'^2 \rangle^{1/2}$
1.95	10.2	28.4	16.8	24.4	16.1	16.8	4.6
1.95	20.4	27.8	17.5	22.4	16.1	24.1	9.1
1.95	51.0	22.4	15.3	18.3	14.6	21.9	5.0
10.66	10.2	75.0	57.3	69.5	55.7	7.9	2.71
10.66	20.4	66.8	55.5	61.0	53.0	9.5	4.6
10.66	51.0	48.5	39.6	47.2	36.6	2.6	8.3

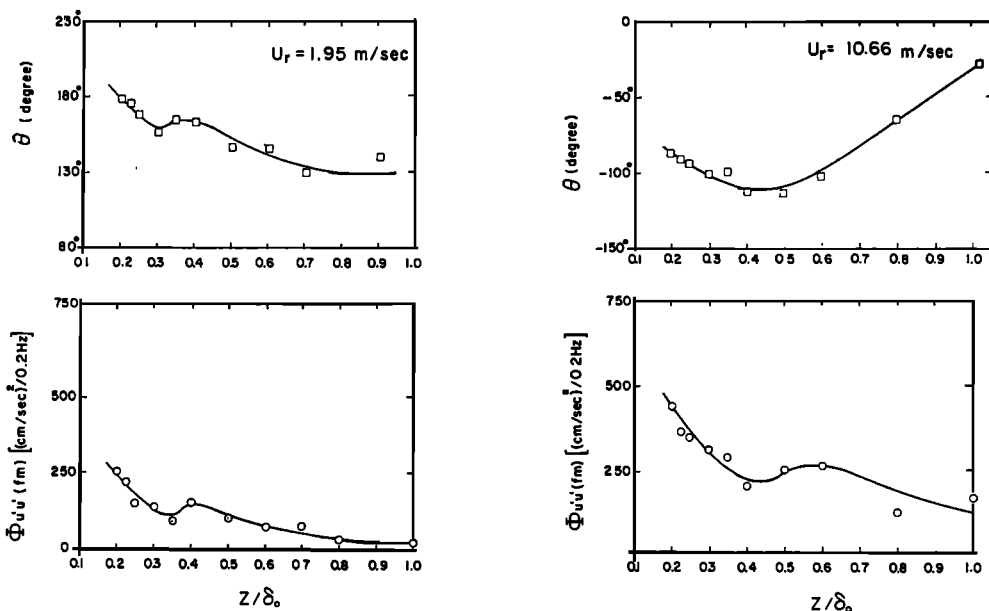


Fig. 11. Profiles of power spectrum $\Phi_{u'u'}(f_m)$ and phase shift θ at fetch 9.15.

by assuming that K_p is zero in the absence of wind. Assuming further that the same damping factor remains in the presence of wind, the growth factor K_g is obtained. Both of the above assumptions are not always true. Evidence given by *Harris* [1966] on the wave driven wind indicates that some wave damping

due to aerodynamic effects must take place even in the absence of a gradient wind. Also, the presence of surface contaminants may be less severe with wind than without wind. The above assumptions are, nevertheless, considered reasonable and the growth and damping rate factors are estimated from spectral measurements

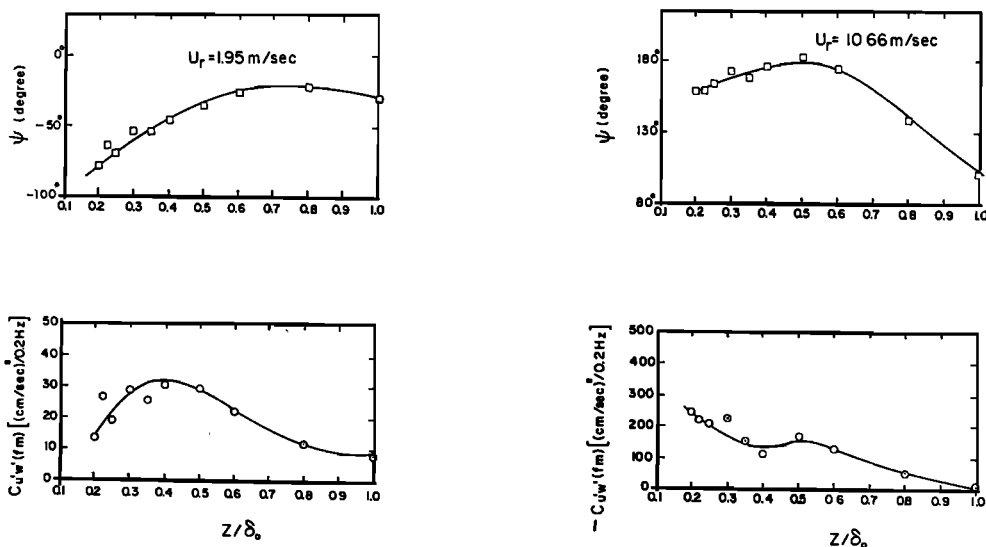


Fig. 12. Profiles of co-power $C_{u'w'}(f_m)$ and phase shift ψ at fetch 9.15.

at fetches 9.15 and 24.36. The results are summarized in Table 4.

Interesting observations follow from the results in Table 4. The most obvious is that the spectral values at the mechanical wave frequency decrease with increasing wind speed at each fetch. This is attributed to the wind-generated current which increases the group velocity of the wave system. Measurements of current were reported by *Shemdin and Lai* [1970]. The surface current was found to be 3% of free stream velocity and to be reasonably constant with fetch. Preliminary estimation of the effect of surface current based on triangular and uniform profiles suggested changes in wave energy of the same order of magnitude as observed. An accurate analysis of the interaction of waves with a wind-generated current is being pursued and the details of analysis are beyond the scope of this paper. The results shown in Figure 4 are consistent with theoretical computations. At fetch 9.15, the reduction in wave energy is more noticeable than at fetch 24.36 simply because the reduction in wave energy due to surface current at the latter fetch is compensated for by the energy received from wind over a fetch of 15.21 meters.

The viscous damping factor is found to be $1.1 \times 10^{-2} \text{ m}^{-1}$ and is larger than viscous damping predictions due to channel walls and bottom only; but it is consistent with the theoretical predictions which include, in addition, the viscous effects at the surface as suggested by *Van Dorn* [1966] for what he calls an immobile surface. Our measurements verify the importance of surface effects. The growth factor is much smaller than the damping factor at the low wind speeds and increases to 72% of the damping factor at $U_r = 10.66 \text{ m/sec}$. The wave en-

ergy decreased with fetch at all wind speeds studied.

The growth factor K_g for a particular wave is related by equation 14 to b which represents the normalized out-of-phase component of pressure. This is only true when the growth of wave is entirely due to atmospheric input of energy and the energy transfer is predominantly by normal pressure. These conditions are not strongly violated by mechanical generation of waves in a wind and wave facility. When the generation of waves is strictly by wind energy, transfer also takes place by nonlinear interactions between the different wave components in the spectrum and equation 14 becomes invalid. Pressure measurement above mechanical waves were reported by *Shemdin and Hsu* [1967] and by *Shemdin* [1969a]. The b values were calculated from pressure measurements in the latter study and compared with *Miles's* [1959] theory. The b values computed from growth rate of waves, as shown in Table 4, are compared with those reported by *Shemdin* [1969a] in Figure 13. The agreement is considered reasonable.

Ideally the computation of growth rate of waves needs to be compared to the momentum transfer to waves obtained by cross correlation of u' and w' measured by sensors which follow the waves and remain close to the interface at all times. Denoting the fluctuating velocity field in the absence of mechanical waves by (u'' , v'' , and w'') and the total fluctuation in the presence of mechanical waves by (u' , v' , and w')

$$u' = U + u'', v' = v'',$$

and

$$w' = W + w'' \quad (16)$$

TABLE 4. Growth and Decay Factors of Waves
 $k = 1.92 \text{ m}^{-1}$; $c = 2.23 \text{ m/sec}$.

U_r , m/sec	Fetch 9.15 $\Phi_{\eta\eta}(f_m) \times 10^3$, $\text{m}^2/0.2 \text{ Hz}$	Fetch 24.36 $\Phi_{\eta\eta}(f_m) \times 10^3$, $\text{m}^2/0.2 \text{ Hz}$	R	$(K_g - K_v)$ $\times 10^3 (\text{m}^{-1})$	K_g $\times 10^3 (\text{m}^{-1})$	b
0	1.07	0.901	0.845	11.0	0	0
1.95	1.04	0.883	0.855	10.2	0.69	0.18
2.86	0.957	0.855	0.892	7.45	3.54	0.925
4.57	0.93	0.819	0.875	8.76	2.85	0.745
6.10	0.892	0.781	0.880	8.40	2.95	0.77
10.66	0.696	0.66	0.954	3.08	7.93	2.02

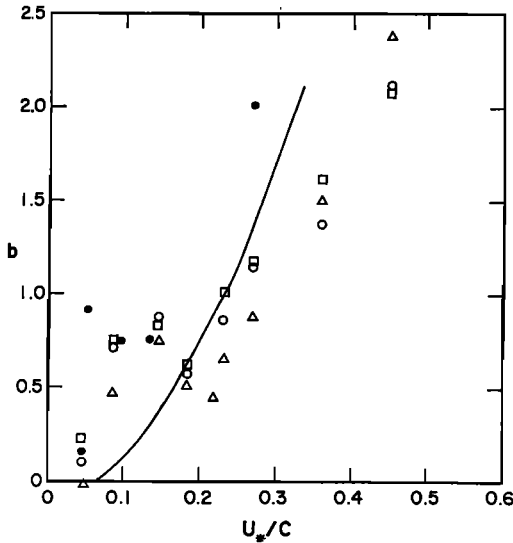


Fig. 13. Comparison between b values from wave growth rate measurements and from direct measurements of pressure. Triangles, $a_0 = 3.17$ cm; squares, $a_0 = 5.38$ cm; open circles, $a_0 = 8.00$ cm; frequency = 0.78 Hz; pressure measurements: *Shemdin* [1969a]. Closed circles, wave growth measurements; dashed lines, *Miles's* [1959] theory.

where (U, W) denote the wave induced velocity field. The rate of momentum transfer F was given by *Phillips* [1966]

$$F = -\rho_a \left[\langle UW \rangle + \left\langle u'^2 \right\rangle \frac{\partial \eta}{\partial x} \right] \quad (17)$$

the subscript s denotes evaluation at surface, the first term on the righthand side represents the wave induced stress and the second term represents the contribution of turbulence to momentum transfer. Turbulent measurements from a frame of reference which follows the water surface are not available for evaluation of F according to equation 17.

The results of this study may be used to estimate the wave-induced stress from a fixed frame at a small elevation ($z = 10.2$ cm) above the crest level. Interesting conclusions about turbulence can be derived by comparing the wave-induced stress to the rate of transfer of momentum obtained from wave growth measurements. Defining b_w as (equation 6)

$$b_w = \frac{-\langle UW \rangle}{gk \left(\frac{a_0^2}{2} \right)} \quad (18)$$

it is found that $b_w = 0.8$ for $U_w = 10.66$ m/sec at fetch 24.36, and from Table 4 $b = 2.02$ for the same wind speed. The comparison suggests that the turbulent contribution to momentum similar to the second term on the righthand side of equation 17 is significant compared to the wave-induced stress. Similarly for $U_w = 1.95$ m/sec and fetch 24.36, it is found that b_w is negative while $b = 0.18$ from Table 4. This can only be true if the turbulent contribution to momentum transfer (positive) exceeds the wave-induced stress (negative) to produce wave growth. It is therefore concluded that perturbation of turbulence in air by surface waves produces significant momentum transfer in addition to the wave-induced stress.

CONCLUSIONS

The following conclusions are derived for simple propagating waves in wind-wave channels:

1. The wave-induced perturbations (organized motion) are significant compared to turbulent fluctuations (random motion) in the air flow and play a role in momentum transfer from air to water.
2. Future theoretical formulations to describe the flow above the air-sea interface should include the nonlinear terms $U_i U_j$, where U_i and U_j represent the wave-induced perturbations in the air flow.
3. The wave-induced perturbations decay with elevation and the rate of decay depends on wind speed compared to wave speed.
4. The magnitude and direction of the wave-induced stress above the crest depends critically on $(U_1 - C)$. The direction of stress is upward when $U_1 < C$.
5. Further analysis of data is necessary for use in numerical models. The description of the velocity field in terms of organized and unorganized motion is desirable and is being pursued. Measurements of turbulent fluctuations immediately above wavy surface (in trough) are needed to evaluate contributions of organized and unorganized motions to wave growth.

Acknowledgments. This investigation was conducted in the Coastal and Oceanographic Engineering Laboratory at the University of Florida. The analog power-spectrum analyzer was provided by the College of Engineering. The authors acknowledge the assistance of Messrs. R. M. Batey,

A. J. Evans, and P. M. Lin. The work was sponsored by the National Science Foundation under grant GK-3986 and by the Coastal Engineering Research Center under grant DACW72-69-C-0019.

REFERENCES

- Champagne, F. H., and C. A. Sleicher, Turbulence measurements with inclined hot-wires, part 2, *J. Fluid Mech.*, **28**, 176-182, 1967.
- Champagne, F. H., C. A. Sleicher, and O. H. Wehrmann, Turbulence measurements with inclined hot-wires, part 1, *J. Fluid Mech.*, **28**, 153-175, 1967.
- Deardorff, J. W., Aerodynamic theory of wave growth with constant wave steepness, *J. Oceanogr. Soc.*, **23**, Japan, 282, 1967.
- Harris, D. L., The wave driven wind, *J. Atmos. Sci.*, **23**(6), 688-693, 1966.
- Hess, G. D., G. M. Hidy, and E. J. Plate, The structure of turbulence in air flowing over small water waves, *NCAR Manuscript 68-79*, Boulder, Colo., 1968.
- Karaki, S., and E. Y. Hsu, An experimental investigation of the structure of a turbulent wind over water waves, *Dept. of Civil Eng. Tech. Rep. 88*, Stanford University, Stanford, 1968.
- Kato, H., and K. Sano, Measurements of wind velocity fluctuations over waves in a wind-wave tunnel, *Rep. Port and Harbor Res. Inst. 8*, Yokosuka, Japan, 1969.
- Kendall, J. J., Jr., The turbulent boundary layer over a wall with progressive surface waves, *J. Fluid Mech.*, **41**, 259-281, 1970.
- Klatt, F., The X hot-wire probe in a plane flow field, *Disa Information*, **8**, 3-12, Harlev, Denmark, 1969.
- Liu, C. K., S. J. Kline, and J. P. Johnston, An experimental study of turbulent boundary layer on rough walls, *Dept. Mech. Eng. Rep. MD-15*, Stanford University, Stanford, 1960.
- Longuet-Higgins, M. S., A nonlinear mechanism for the generation of sea waves, *Proc. Roy. Soc. London, Ser. A*, **311**, 371-389, 1969.
- Phillips, O. M., On the generation of waves of turbulent wind, *J. Fluid Mech.*, **2**, 417-445, 1957.
- Phillips, O. M., *The Dynamics of the Upper Ocean*, Cambridge University Press, London, 1966.
- Rose, W. G., Results of an attempt to generate a homogeneous turbulent shear flow, *J. Fluid Mech.*, **25**, 97-120, 1966.
- Ruggles, K. W., The wind field in the first ten meters of the atmosphere above the ocean, *Dept. Meteorol. Rep. 69-1*, Massachusetts Institute of Technology, 1969.
- Shemdin, O. H., and E. Y. Hsu, Direct measurement of aerodynamic pressure above a simple progressive gravity wave, *J. Fluid Mech.*, **30**, 403-416, 1967.
- Shemdin, O. H., Instantaneous velocity and pressure measurements above propagating waves, *Dept. Coastal and Oceanogr. Eng. Tech. Rep. 4*, University of Florida, Gainesville, 1969a.
- Shemdin, O. H., Air-sea interaction laboratory facility, *Dept. Coastal and Oceanogr. Eng. Tech. Rep. 3*, University of Florida, Gainesville, 1969b.
- Shemdin, O. H., Wave influence on wind velocity profile, *J. Waterways Harbors Div., Amer. Soc. Civil Eng.*, **96**(4), 795-813, 1970.
- Shemdin, O. H., and R. J. Lai, Laboratory investigation of wave-induced motion above air-sea interface, *Dept. Coastal and Oceanographic Eng. Tech. Rep. 6*, University of Florida, Gainesville, 1970.
- Smith, J. D., Thurst-anemometer measurements of wind-velocity spectra and Reynolds stress over a coastal inlet, *J. Marine Res.*, **25**, 239-262, 1967.
- Stewart, R. W., Mechanics of the air-sea interface, *Physics of Fluids*, **10**(9), S47-58, 1967.
- Van Dorn, W. G., Boundary Dissipation of Oscillatory Waves, *J. Fluid Mech.*, **24**, 769-779, 1966.
- Wu, J., Wind-wave interactions, *Physics of Fluids*, **13**, 1926-1930, 1970.

(Received December 1, 1970;
revised July 22, 1971.)